Environmental Technology & Innovation 32 (2023) 103237

Contents lists available at ScienceDirect

Environmental Technology & Innovation

journal homepage: www.elsevier.com/locate/eti

An evaluation of the feasibility of electrostatic separation for physical soil washing

X. Corres [a], D. Baragaño [b], J.M. Menéndez-Aguado [c], J.R. Gallego [a], C. Sierra [d,e,*]

[a] INDUROT and Environmental Biogeochemistry & Raw Materials Group, Campus de Mieres, Universidad de Oviedo, Mieres, Asturias, Spain
[b] Escuela Politécnica de Ingeniería de Minas y Energía. Boulevard Ronda Rufino Peón nº, 254. Universidad de Cantabria, Torrelavega, Cantabria, Spain
[c] Escuela Politécnica de Mieres. c/Gonzalo Gutiérrez Quirós s/n, 33600, Mieres, Asturias, Spain
[d] Department of Mining, Topography and Structure Technology, University of León, Campus de Vegazana, 24006, León, Spain
[e] European University on Responsible Consumption and Production, University of León, Campus de Vegazana, 24006, León, Spain

ARTICLE INFO

Article history:
Received 17 April 2023
Received in revised form 23 May 2023
Accepted 3 June 2023
Available online 7 June 2023

Keywords:
Potentially toxic elements (PTEs)
Sandy soil
Mineral processing
Lead
Circular economy

ABSTRACT

We present the first application of electrostatic separation for soil washing. Soil samples were collected from the PTE-containing area of La Cruz in Linares, southern Spain. Using a single-phase high-tension roll separator with voltages ranging from 20 kV to 41.5 kV, we achieved yield values between 0.69% and 9%, with high recovery rates for certain elements such as Zn, Cu, and Mo. SEM-EDX analysis revealed three particle types, including a non-conductive fraction composed of feldspar, a middling fraction composed of mica, and a conductive fraction consisting of PTE-bearing slag grains. Attributive analysis showed that 41.5 kV was the optimal voltage for maximizing PTE concentration. Overall, electrostatic separation is a promising approach for treating soils contaminated with PTEs, particularly in dry climate areas impacted by mining activities.

1. Introduction

Potentially Toxic Elements (PTEs) are known to be widespread and present complex challenges due to their failure to decompose, difficulties with remediation, toxicity to plants and in the food chain, and damage to soil ecosystems (Beiyuan et al., 2018; Gu et al., 2018; Li et al., 2019a,b). These pollutants are well-known by-products of human activity, including mining, waste disposal, agriculture, electroplating, and coal combustion (Piccolo et al., 2019; Rui et al., 2019; Wu et al., 2015), thus, soil contamination with PTEs is currently one of the most pressing environmental issues we are faced with. Several million hectares of PTE-contaminated soils are found in Europe alone, accounting for nearly 40% of all contaminated soil worldwide (EEA, 2009). Beyond Europe, this issue affects many other nations, principally the USA (Uchimiya et al., 2011), Japan (Makino et al., 2006), and Brazil (França et al., 2017).

PTE-polluted soils can be remediated using physical (soil replacement, physical soil washing, thermal desorption), chemical (chemical soil washing, solidification/stabilization electrokinetic, vitrification), and biological (phytoremediation, microorganism remediation, animal remediation) (Anderson et al., 1999; Beiyuan et al., 2018; Dermont et al., 2008) treatment methods. Soil washing techniques have their origin in the mining industry and involve either the separation of soils by particle size and density generally using water as the carrier agent (physical washing) or the use of a chemical to

* Corresponding author at: Department of Mining, Topography and Structure Technology, University of León, Campus de Vegazana, 24006, León, Spain.
E-mail address: csief@unileon.es (C. Sierra).

https://doi.org/10.1016/j.eti.2023.103237

extract the contaminant (chemical washing) (Anderson et al., 1999). Such techniques result in a clean fraction that can be backfilled on site and a contaminated fraction that can be disposed of appropriately. In comparison to other methods, physical soil washing is one of the most remarkable decontamination techniques due to its capacity to permanently remove PTEs, fast processing, waste volume reduction, and significant cost/effectiveness ratio (Baragaño et al., 2021, 2023; Feng et al., 2020; Khalid et al., 2017; Wang et al., 2018; Xu et al., 2014; Zhao et al., 2017).

Electrostatic separation makes use of differences in electrical conductivity between minerals (Inculet, 1984) and on the face of it, this method would seem to be a universal method of separation because all materials exhibit some variation in conductivity. In reality, however, it has several limitations, specifically, its low capacity for fine grain sizes, the processing requirement of a dry monolayer feed, limitations with soil sample variability, sensitivity to moisture and moderate to high energy consumption (mainly due to drying) (Kawatra and Young, 2019). Typically, this method is used with granular feeds with particle sizes ranging from 40 μm to 1 mm (Kawatra and Young, 2019).

As discussed in Yang et al. (2018), electrostatic separation is widely used for the recovery of ilmenite ore, rutile, and zircon from sands. It also plays a part in many recycling processes, for example in the separation of metal from plastic in lots of scrap electrical cabling (Bedeković and Trbović, 2020; Park et al., 2015), and in the food industry to isolate or concentrate proteins found in various foodstuffs (Kdidi et al., 2019; Tabtabaei et al., 2017, 2019). In addition, the technique is used in the petrochemical industry for desalting crude oil (Aitani, 2004) and for the purification of certain products (Li et al., 2019a,b, 2021; Villot et al., 2012).

Despite its proven effectiveness in many areas, however, electrostatic separation does not appear to have been investigated as a method for soil decontamination. As stated above, one reason for this may be the fact that this method requires a dry feed. The costs involved in drying soils before processing represent a major obstacle to the use of electrostatic separation in a soil washing operation. The site we are considering in this research, La Cruz in the Linares-La Carolina mining district (Southern Andalusia, Spain), side-steps this problem as its Mediterranean climate means there is little rainfall, and its soils are thus completely dry for most of the year (Lorite et al., 2023). Thus, with its arid climate it is an ideal site to test electrostatic separation of soils.

Following from the discussion above, the primary goals of the current study are:

- To evaluate the feasibility of electrostatic separation as part of physical soil washing treatments for soils containing PTEs.
- To explain the underlying aspects of the separation by means of a detailed mineralogical study.
- To test a novel formulation (attributive analysis) for the assessment of separation efficiency and thus determine optimal separation conditions.

2. Materials and methods

2.1. Site description

Galena (PbS) has been mined at La Cruz for over two centuries making it one of the most important led ore mining regions in the world (Lillo Ramos, 1992; Martínez et al., 2007b,a, 2012). The led ore is found in veins with sphalerite (ZnS), chalcopyrite ($CuFeS_2$), and barite ($BaSO_4$) thus processing and extracting the useful ore creates a significant quantity of waste which is often dumped on the land next to mining operations. Moreover, much of the mineral processing at the site considered here involved gravity separation and froth flotation resulting in both medium and fine grain rejects that were then sent to nearby landfills or dumps. In addition, the solid, liquid, and gaseous contaminants produced by the district's foundries remain on these sites in the form of slag and dust, an environmental problem discussed by Adamo et al. (1996) and Li and Thornton (2001) at similar sites in Canada and the UK, respectively. When these industrial residues, containing fractions with a high concentration of heavy metals, are dispersed and dumped on the ground without any prior remediation treatment the action of weathering increases their chemical availability (Loredo et al., 1999; Martínez et al., 2007a) making them even more environmentally hazardous. In this way, mining waste in all its forms constitutes a significant problem for the extensive agricultural areas of the zone (Sierra et al., 2013). Location map is presented in SM1. According to Heliosat (SARAH), the study site receives an average of 3.3 h of sunlight per day, with 5.82 peak sun hours (PSHs) and an average annual solar radiation of over 5 kwh/m^2 on a horizontal surface (H) (e.g., Pfeifroth et al. (2017)). Based on this information, it is evident that solar energy can serve as a viable alternative energy source to power the electrostatic separation process.

2.2. Sample preparation

Samples were taken from 10 randomly selected sites across the location of interest. All samples were taken from the top 35 cm layer of soil; the depth was measured using a stainless-steel calliper and a shovel was used to collect the sample. In total a bulk sample of 25 kg was collected. The sample was then homogenized and kept at room temperature in inert plastic containers until further preparation and analysis. All soil analysis was completed within 15 days of the initial sampling.

The bulk sample was wet sieved in batches for five minutes with a water flow of 0.3 l/min to obtain granulometric fractions of 63, 63–125, 125–250, 250–500, 500–1000, and 1000–2000 μm (ASTM D-422-63, Standard Test Method

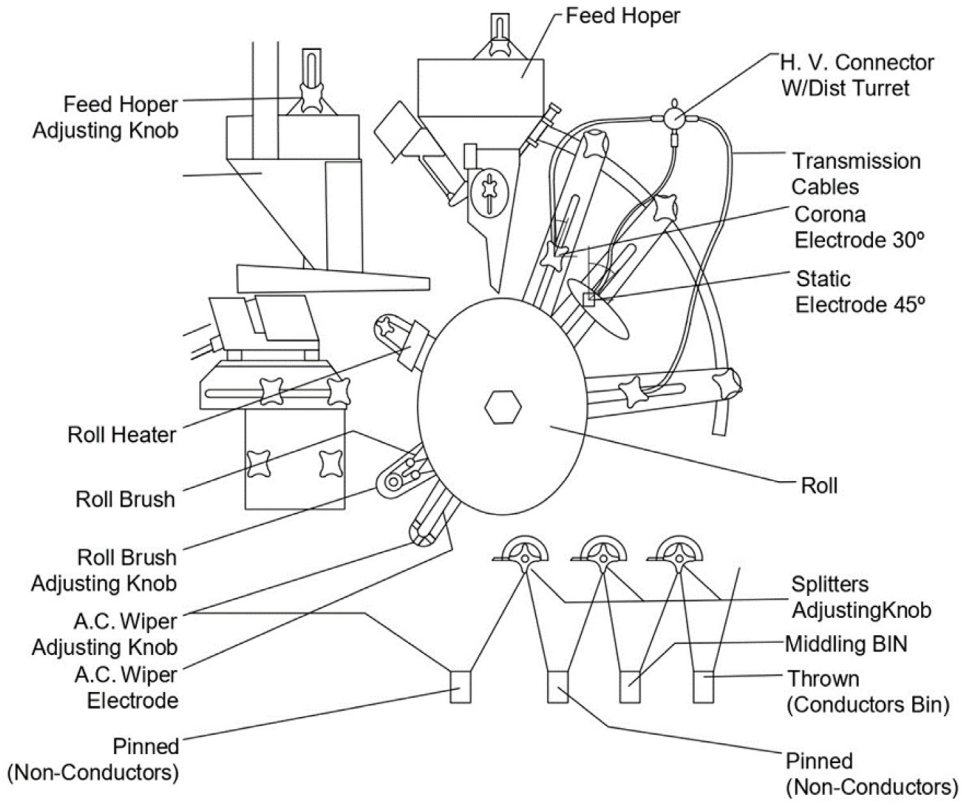

Fig. 1. Scheme of the high voltage electrostatic separation process.

for Particle-Size Analysis of Soils). Note that, sodium hexametaphosphate and sodium carbonate were used to aid the separation of the silt-clay fraction (<63 μm) from the larger particles. The process was repeated until 3 kg of the 1000–2000 μm fraction was obtained. This fraction was divided into twelve subsamples, which were reserved for further processing in the electrostatic separator. Additional subsamples were taken from each fraction, and these were air dried at 40 °C before being sent for chemical analysis.

2.3. Electrostatic separation

As described above, twelve samples were made from the 1–2 mm fraction of soil collected from the site of interest. Each sample was tested at a different separation voltage with experimental runs at each voltage repeated three times. An average of these results was taken and is presented in this article. The apparatus used was an eForce high voltage electrostatic separator (model EHTP by Outotec) (Fig. 1 and SM2) which is one the few semi-industrial electrostatic separators operating in Europe.

The apparatus employed has the following design characteristics:

- Feed particle size range: 0.074–10 mm.
- Treatment capacity: up to 150 kg/h.
- Vibratory tray and hopper with variable speed control for coarser particles and a positive speed feed chute and vibrator hopper for finer particles.
- Hopper with 2 adjustable dividers for the collection of non-conductive, intermediate (middling), and conductive products.
- 2 interchangeable stainless-steel rollers:
    - Of sizes 25.4 and 35.56 cm (10 and 14″) in diameter by 15.24 cm (6″) wide (industry standards) and
    - Of variable roll speed with a 1/4 HP direct drive motor.
- 2 DC electrodes, one corona and the other static, which can be set at a range of voltages to a maximum of 41.5 kV; and 1 AC wiper electrode at 18 kV.
- High voltage transformer, adjustable up to 12,000 VAC.

- Grounded roller brush for particle removal: adjustable and with infrared roller heating capability.

The module was operated under the following conditions:

- Corona electrode angle: 30° with respect to the vertical.
- Electrostatic electrode angle: 45° with respect to vertical.
- Roll speed: 50 rpm.

Samples were fed into the feed hopper and onto the roller. The corona electrode ionizes the surrounding air and charges the particles on the roller as they approach the electrode. Conductive particles lose their charge quickly to the earthed roller and are thrown into the conductors bin due to the centrifugal force of the roller. The more insulating particles retain their charge and will stay on the roller until they are brushed off and fall into either the middlings or insulators bin (depending on particle size and roller speed).

The degree of separation that can be achieved for a given sample will depend on the composition of the sample, roller speed, electrode positions, and separation voltage (the voltage of the corona electrode). In this work, the only variable was the separation voltage which was set at a range of values from 20 kV to 41.5 kV in order to determine the optimum voltage for the soils sampled here.

2.4. Chemical and mineralogical analysis

Before chemical analysis, subsamples (6 from the grain size fractioning and 108 from the separation experiments) needed to be standardized thus, all fractions >125 μm were milled using a vibrating disk mill (RS 100 Retsch) at 400 rpm for 40 s Then, representative samples of 1 g were taken from each subsample, and these were subjected to "Aqua regia" ($HCl + HNO_3$) digestion before being sent for ICP-OES analysis at the ISO 9002 accredited laboratories, Actlabs International (Ancaster, Ontario, Canada). Tests returned the total concentrations of the following 36 major and trace elements: Ag, Al, As, Au, B, Ba, Bi, Ca, Cd, Co, Cr, Cu, Fe, Ga, Hg, K, La, Mg, Mn, Mo, Na, Ni, P, Pb, S, Sb, Sc, Se, Sr, Te, Th, Ti, Tl, V, W, Zn. Samples that exceeded the limit of quantification for the previous method (13 in total) were treated in triplicate with Fusion-Inductively Coupled Plasma-Sodium Peroxide Oxidation (FUS-Na_2O_2) in the same laboratories. This process involves sintering the sample at 650 °C after oxidizing it with sodium peroxide. The resulting oxidized material was then dissolved in aqueous HNO_3, and various elements in the resulting solution are quantified using ICP-OES (report number: A19-03313).

The subsamples were also examined using a stereoscopic binocular microscope (Nikon SMZ1000) and micrographs were obtained with a high-resolution Nikon DS-Ri1 camera. The morphology and composition of minerals was examined using an SEM-EDX system, comprising a Jeol JSM-6100 scanning electron microscope and an energy dispersive X-ray analyser (INCA Energy 200).

3. Results and discussion

3.1. PTEs concentration in soils

Nine PTEs tested for in this study (As, Cd, Cu, Cr, Hg, Ni, Pb, Sb, and Zn), were found in quantities above the target limits set by current international standards (Buchman and Office of Response, 2008) and three (Cu, Zn, Pb) were significantly above both the intervention limit (Table 1), and the contamination ratio (CR: the quotient of sample concentration and the target value for the element of interest). The concentration of Mo in the soil samples was determined to be below the reference levels. Nevertheless, it was included in the study due to its geochemical importance and economic significance, as well as its notable performance in the separation process. Furthermore, the analysis also incorporated Al and Fe due to their high conductivity. Cu was the most significant soil PTE at the site of interest (176.13 mg/kg to 802.32 mg/kg, mean: 362.7 mg/kg; CR: 106.68) followed by Zn (376.06 mg/kg to 2375.37 mg/kg, mean: 1051.03 mg/kg; CR: 65.69), and, as expected, Pb (1620.25 mg/kg to 3455.43 mg/kg, mean: 2412.81 mg/kg; CR:43.87). Another PTE, As was found to have a CR of similar order to the main 3 PTEs (53.84). In this way, there is a major case for a soil decontamination programme at the site of interest focusing principally on Cu, Zn, and Pb but which might be extended first to As, and later to Ni, Cr, Cd, Sb, and Hg. The soil exhibited a sandy loam texture, like many soils found in Mediterranean regions.

3.2. Electrostatic separation

The results of electrostatic separation were initially assessed according to three standard ore processing parameters: yield (γ), recovery (ε), and enrichment ratio (μ) (Wills and Napier-Munn, 2006). The yield or weight recovery is the quotient of the feed mass and that of the conductive fraction collected for a given experimental run. The recovery is the quotient of the mass of an element of interest found in the conductive fraction and that of the feed for a given experimental run. Finally, the enrichment ratio is the quotient of the concentration of an element of interest found in the conductive fraction and that of the feed for a given experimental run.

Table 1
PTEs concentrations in the bulk sample, the international standard (target and intervention limits), and contamination ratio for each PTE tested for in addition to Al, Mo and Fe. Elements marked with an asterisk are those with concentrations surpassing both the intervention and target values.

Element	Concentration (mg/kg)	Dutch standards (mg/kg) (Buchman and Office of Response, 2008)		Contamination ratio
		Intervention	Target	
Al	4681.2	–	–	–
As	48.46	55	0.9	53.84
Cd	7.48	12	0.8	9.35
Cr	10.41	220	0.35	29.75
Cu*	362.70	96	3.4	106.68
Fe	19 590.53	–	–	-
Hg	0.76	10	0.3	2.54
Mo	1.71	115	190	3
Ni	9.17	100	0.26	35.28
Pb*	2412.81	530	55	43.87
Sb	11.96	15	3	3.99
Zn*	1051.03	350	16	65.69

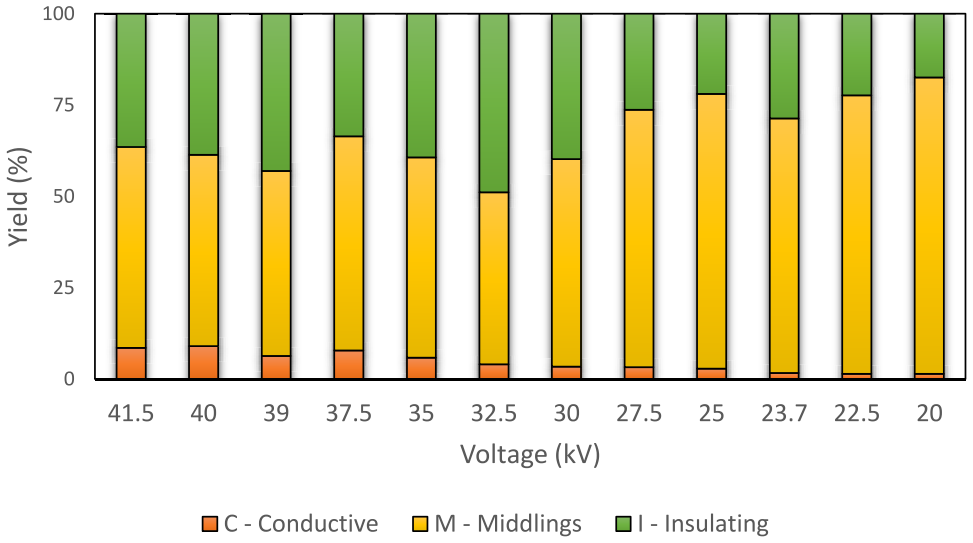

Fig. 2. Yield (γ) distribution between fractions for experimental runs.

Experimental runs were completed for 12 values of corona electrode voltage starting with the highest voltage available (41.5 kV). The voltage was gradually reduced on each subsequent run to determine the optimal operating conditions. At all voltages, we observed lowest yields ($\gamma = 0.69\% - 9\%$) for the conductive fraction compared to the middlings ($\gamma = 50.68\% - 90.59\%$) and insulating fraction ($\gamma = 8.72\% - 48.89\%$) (Fig. 2).

Looking in detail at the relationship between the yield for the conductive faction and applied voltage, here we found a positive correlation: the higher the voltage, the higher the yield with an almost directly proportional relationship (SM3). This suggests that higher voltages increased the number of conductive particles collected from the feed. However, higher voltages may also increase the capture of insulating particles, which could reduce recovery, and this highlights the need for more exhaustive study into the selection of an optimal operating voltage.

For most PTEs, the enrichment ratio, μ, is lower for the middlings and insulating fractions (<1% in all cases) compared to the conductive fraction (Table 2). This is a reflection of the fact that most pollutants tested here were metallic or semi-metallic and thus would be expected to report to the conductive fraction.

No clear tendencies were seen with respect to the enrichment ratios for any of the separated fractions (insulating, middlings, or conductive) and voltage. Considering the specific elements of interest (Fig. 3), here it can be seen that while some reached their highest enrichment ratio in the lower voltage range (e.g., Cu had $\mu = 7.49$ at 20 kV in contrast with an $\mu = 7.26$ at 41.5 kV), others exhibited the converse relation (e.g., Sb had $\mu = 9.15$ at 39 kV compared to $\mu = 4.54$ at 22.5 kV).

As with the yield, recovery (ε) in the conductive fraction also demonstrated a clear, positive correlation with voltage. Considering the recovery of individual elements, here Zn removal was the most successful, with recovery values of about 80% for voltages from 37 kV to 41.5 kV. The maximum recovery value for this element was 83.25% with a yield, $\gamma = 9$ %, at an operating voltage of 40 kV. Recovery for this element decreased abruptly at 37 kV, a pattern seen for all 10 elements studied (Fig. 4). Referring back to Fig. 3 we see that the enrichment ratio for this element was high and varied very little

Table 2
Partial merit index (Q_j^i), adjusted correction factor ($A_j^{i'}$) and global merit index ($\boldsymbol{Q_T^i}$) for each experiment (i) and element (j).

	Tens. (kV)	j																			Q_T^i
		As		Cd		Cr		Cu		Hg		Mo		Ni		Pb		Sb		Zn	
		Q_j^i	$Q_j^i A_j^{i'}$	Q_j^i	$Q_j^i A_j^{i'}$	Q_j^i	$Q_j^i A_j^{i'}$	Q_j^i	$Q_j^i A_j^{i'}$	Q_j^i	$Q_j^i A_j^{i'}$	Q_j^i	$Q_j^i A_j^{i'}$	Q_j^i	$Q_j^i A_j^{i'}$	Q_j^i	$Q_j^i A_j^{i'}$	Q_j^i	$Q_j^i A_j^{i'}$	Q_j^i	$Q_j^i A_j^{i'}$	
i	41.5	1.013	0.092	0.921	0.106	0.926	0.080	0.881	0.094	0.636	0.104	1.081	0.185	1.081	0.111	0.997	0.111	1.081	0.108	1.059	0.176	1.142
	40	1.077	0.096	1.077	0.095	1.003	0.076	1.041	0.129	0.588	0.085	1.060	0.165	1.015	0.089	1.077	0.089	1.019	0.094	1.077	0.173	1.089
	39	1.037	0.075	0.758	0.067	0.843	0.053	1.109	0.125	0.622	0.083	1.032	0.102	0.790	0.039	1.044	0.039	1.080	0.078	1.104	0.118	0.818
	37.5	1.069	0.093	0.852	0.074	1.088	0.092	0.973	0.159	1.088	0.113	1.063	0.112	0.951	0.098	1.061	0.098	1.066	0.103	1.081	0.134	1.067
	35	0.842	0.052	0.725	0.046	0.788	0.054	0.911	0.055	0.536	0.042	0.913	0.066	0.861	0.046	0.725	0.046	0.767	0.054	1.008	0.078	0.559
	32.5	0.722	0.049	0.617	0.039	0.766	0.043	0.643	0.039	0.602	0.032	0.845	0.050	0.865	0.053	0.584	0.053	0.493	0.053	0.959	0.053	0.469
	30	0.616	0.041	0.628	0.044	0.587	0.041	0.647	0.052	0.613	0.035	0.812	0.051	0.754	0.050	0.758	0.050	0.699	0.047	0.866	0.051	0.467
	27.5	0.506	0.040	0.471	0.038	0.536	0.046	0.643	0.041	0.681	0.030	0.620	0.041	0.494	0.040	0.594	0.040	0.510	0.036	0.697	0.043	0.402
	25	0.443	0.034	0.589	0.049	0.379	0.049	0.533	0.027	0.484	0.020	0.550	0.032	0.379	0.033	0.514	0.033	0.452	0.031	0.675	0.035	0.339
	23.7	0.535	0.037	0.610	0.036	0.521	0.040	0.527	0.020	0.574	0.023	0.622	0.017	0.471	0.055	0.556	0.055	0.561	0.027	0.668	0.018	0.302
	22.5	0.603	0.038	0.648	0.048	0.646	0.039	0.605	0.029	0.663	0.020	0.614	0.030	0.603	0.042	0.614	0.042	0.585	0.031	0.679	0.025	0.334
	20	0.592	0.043	0.631	0.036	0.615	0.038	0.807	0.029	0.565	0.039	0.697	0.023	0.768	0.036	0.623	0.036	0.612	0.036	0.696	0.023	0.341

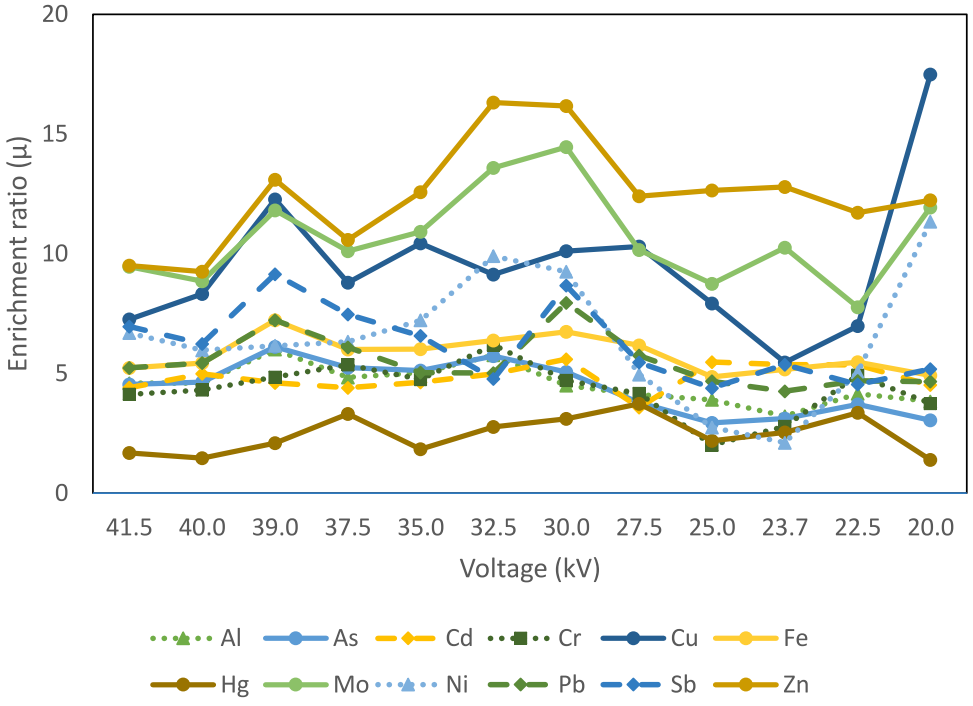

Fig. 3. Enrichment ratio in the conductive fraction for each PTE (plus Al and Fe). Average of three experimental runs at each voltage with a standard error <5%.

with voltage (9 to 16%). Taking 39 kV, in the middle of this high-recovery range, the enrichment ratio $\mu = 13.09\%$ for which $\gamma = 6.33\%$ and $\varepsilon = 82.86\%$.

Mo concentrations in the soil tested were below reference levels, however, we mention it here as its recovery levels were almost as high as those seen for Zn (see Fig. 6). That this method appears to be highly effective at separating this particular PTE is significant due to Mo's geochemical importance and economic interest.

The third best recovery values were recorded for Cu, the most important PTE in the soil tested. The maximum recovery value was 77.65% and this was achieved at 39 kV where the enrichment ratio recorded was 12.27%. As for the other PTE's examined here, the best results came at the highest voltages, with recovery values decreasing rapidly at lower voltages.

Regarding Sb, Ni and Pb, the maximum recovery values for these PTEs were 59.65% (41.5 kV), 53.73% (41.5 kV), and 48.92% (40 kV), respectively (Fig. 5). At these high voltages, the enrichment ratios for these elements were between 5 and 9%. As with the other elements tested, recovery fell dramatically at lower voltages.

Satisfactory yields were also obtained for Cd, Cr, and As, for which the maximum recovery values were 44.97% (40 kV), 41.85% (37.5 kV), and 41.75% (40 kV) respectively, with enrichment ratios ranging from 4 to 6%. Mercury was the lowest yielding element in these experiments with a maximum recovery value of 25.88% (37.5 kV) and a corresponding enrichment ratio of 3.31%. Total concentrations results after the separation are presented in SM4.

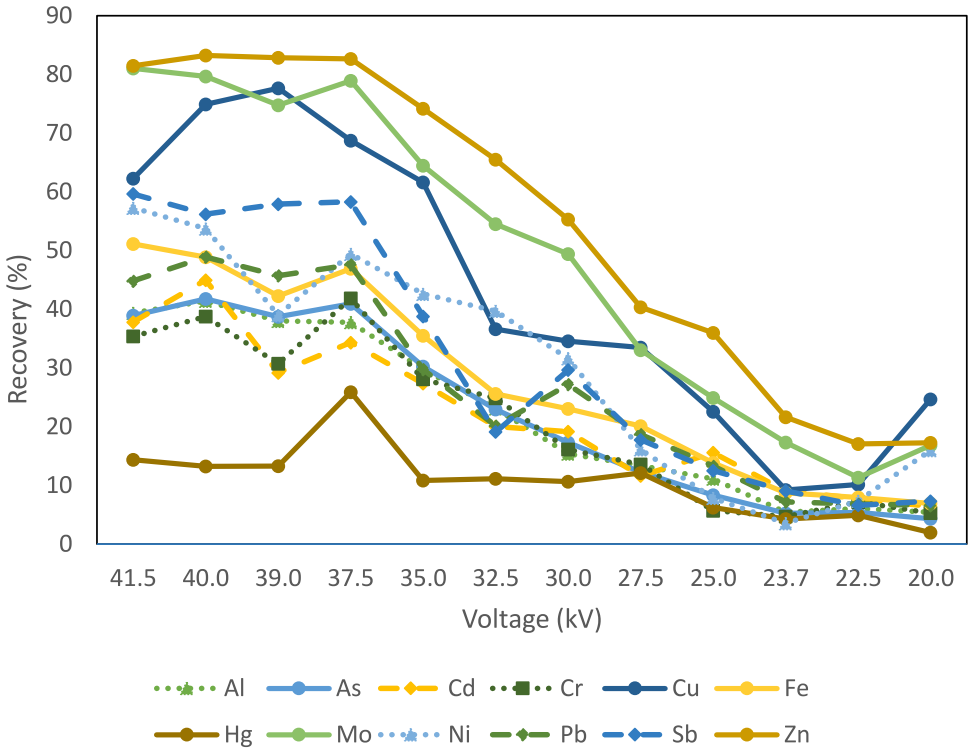

Fig. 4. Recovery in the conductive fraction for each PTE (plus Al and Fe). Average of three experimental runs at each voltage with a standard error <5%.

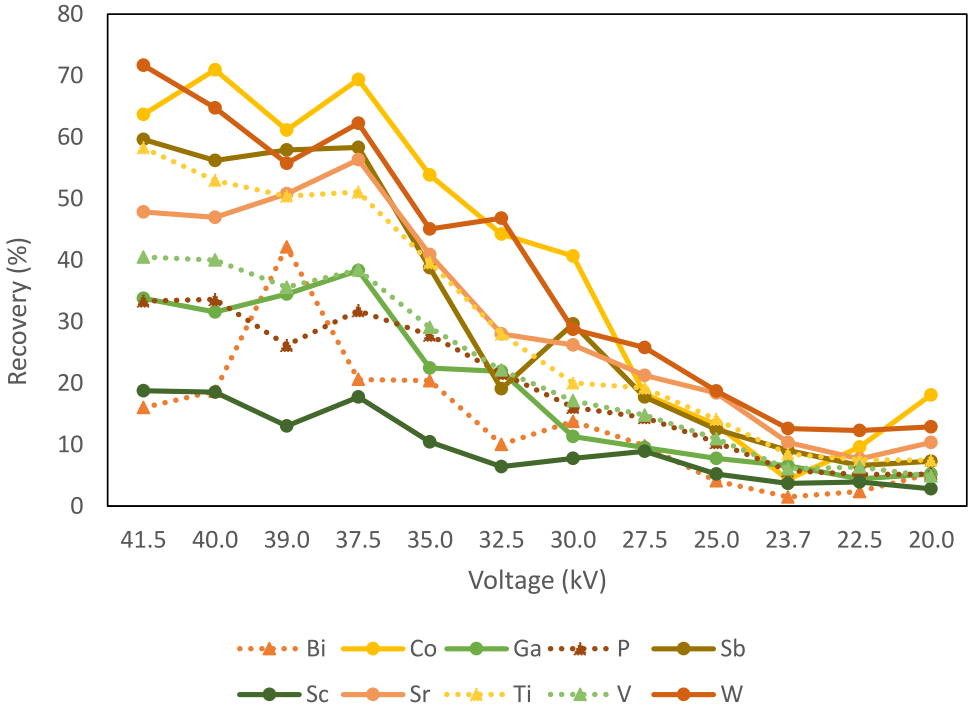

Fig. 5. Recovery of PTEs with significant economic value. Average of three experimental runs at each voltage with a standard error <5%.

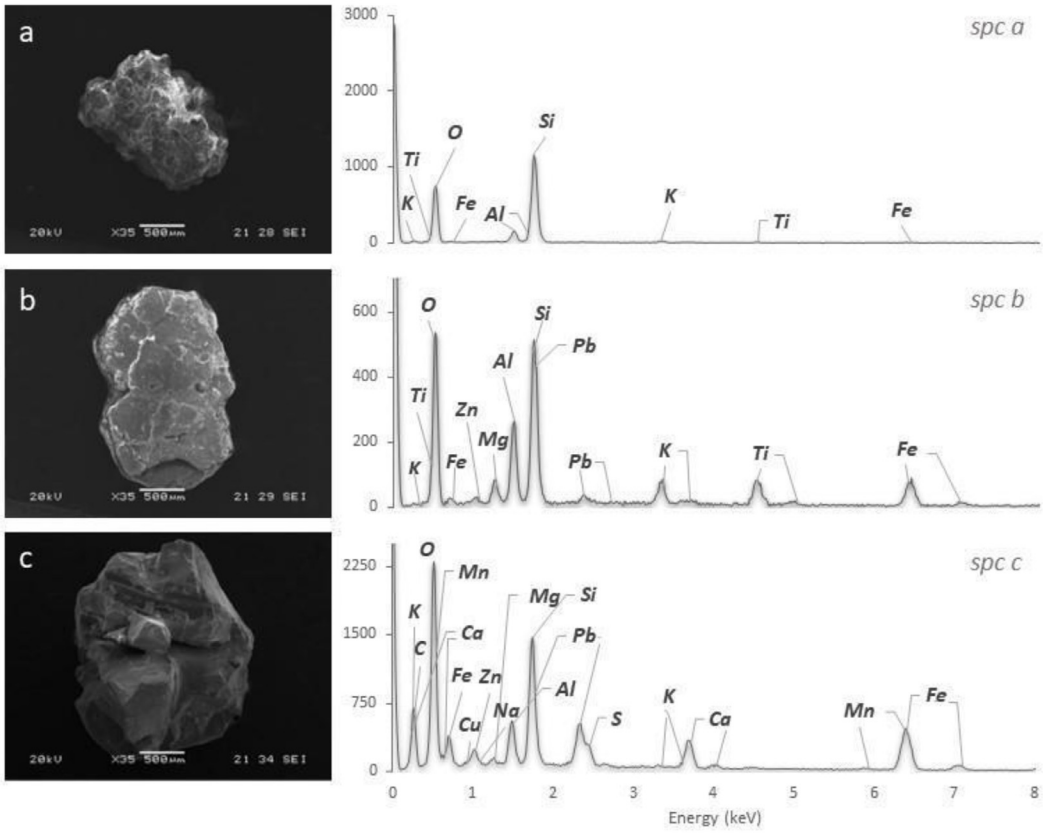

Fig. 6. Selected SEM images of each of the three predominant particle species present in soil fractions obtained after electrostatic separation with representative EDS spectra. (a) Feldspar particle found in the insulating fraction, (b) mica particle found in the middlings fraction, and (c) slag particle found in the conductive fraction.

3.3. Mineralogical analysis of the separated fractions

In order to evaluate the electrostatic separation method from a mineralogical point of view, the three fractions generated were examined under a binocular microscope. In this way, three main types of particles were identified (species 1, 2, and 3) and these were manually separated and studied using SEM-EDX to determine their mineralogical composition. Species 1 (spc.1) particles were found in the insulating fraction (nonconductive material) and were identified as feldspar (Fig. 6a). Further analysis revealed that these particles (Fig. 6, spc. a) were not pollutant bearing, suggesting a geogenic origin for the feldspar in these soil samples. Species 2 (spc. 2) type particles were found to be mica (Fig. 6b), and these were present in highest abundance among the middlings fraction. Analysis of the chemical composition of these particles revealed the presence of Pb and Zn, although in low concentrations (Fig. 6b, spc b). Finally, the most abundant particle in the conductive fraction (Fig. 6c), species 3 (spc. 3), corresponds to the slags identified in previous work on other soils in the region surrounding the site sampled here (Sierra et al., 2013). The presence of Cu, Pb, and Zn in conjunction with high levels of Fe, O, and S (indicating iron oxides and sulphides) points to the existing mineralization and/or mining and metallurgy activities as possible origin of these elements.

3.4. Selecting the conditions for optimal soil washing

We applied the technique of attributive analysis to our experimental results to determine the optimal experimental conditions (specifically the voltage used) for soil washing by electrostatic separation. This technique was designed by Sierra et al. (2010) and details of its derivation can be found in that article. Attributive analysis calculates a merit index (Q) for each experimental test based on the main parameters involved in the mineralogical concentration process thereby enabling tests to be ranked according to their effectiveness.

Optimal separation minimizes yields while at the same time maximizing recovery values. Thus, the merit index of experiment i (where $i = 1, 2, \ldots m$ representing each of the experimental voltages) with respect to PTE j (where $j = 1, 2,$

…n representing each of the PTEs tested) is as follows:

$$Q_j^i = \frac{Min\{\gamma\}}{\gamma^i} + \frac{\varepsilon_j^i}{Max\{\varepsilon\}_j} \tag{1}$$

where:

- γ^i: Yield of experiment i.
- ε_{Ct}^i: Recovery value for the PTE j in experiment i.
- Q_j^i: Merit index for experiment i with respect to element j.

Of course, we wish to find a merit index that takes into account a particular experiment's performance across all elements of interest. However, we cannot simply add the individual merit indices for each experiment and element, since firstly, not all pollutants are equally abundant, and secondly, they each have very different maximum limits. Thus, a weighting factor, A, had to be introduced for each PTE (Eqs. (2), (3)):

$$A_j^i = \frac{\alpha_j^i}{TV} \tag{2}$$

$$A_j'^i = \frac{A_j^i}{\sum_i^m TV_j} \tag{3}$$

where:

- α_j^i: Grade of the feed for the test i and element j.
- TV_j: Target value (international standard, see Table 1) for element j.
- A_j^i: Correction factor.
- $A_j'^i$: Adjusted correction factor.

Finally, the global merit index for each experiment was calculated as follows (Eq. (4)):

$$Q_T^i = \sum_{j=1}^{n} Q_j^i A_j^{i\prime} \tag{4}$$

In this way, we have an indicator of how effectively each experimental voltage achieved separation: minimizing yield and maximizing recovery for each PTE taking into account its individual target levels. The results obtained using this formula for each voltage and PTE are shown in Table 2. It can be observed that higher voltages produce higher merit indices, indicating that broadly, higher voltages lead to more effective separation suggesting that these are the best operating conditions. Attributive analysis of this sort is expected to give an absolute maximum on the side of higher recoveries (41.5 kV) and thus, we conclude that, for optimal one-step separation, 41.5 kV is the best operating voltage.

4. Conclusions

Soils in regions with a history of mining and metallurgy often contain high levels of PTEs that require treatment. In this study, we treated soil samples taken from the La Cruz site in the Linares-La Carolina mining district. This sandy loam soil, typical of the Mediterranean region, contained significant levels of several PTEs, particularly Cu, Zn, and Pb.

Physical and chemical soil washing are well-established remediation strategies for PTE-contaminated soils. Electrostatic separation offers the possibility of separating virtually any mix of materials provided there is enough conductivity difference between components in that mix. Thus, we feel electrostatic separation should be considered among the available tools for soil separation in soil washing operations. The main limitation of electrostatic separation is the need for low moisture levels in the feed and thus the high cost that would be entailed in drying soils before processing. Fortunately, due to the local climate conditions of the site studied here, the soil to be treated was entirely dry.

The results presented here prove that electrostatic separation is a potentially useful tool for decontaminating the coarser fractions of sandy, dry, slag containing soils. In addition, the semi-industrial rig used in this investigation offers the immediate possibility of scaling up operations. The yields obtained in this work ranged from 0.69% to 9% with high recovery values for three PTEs: Zn (83.25%), Cu (77.65%), and Mo (81.01%); and significant recovery levels for six others: Sb, Pb, As, Ni, Cr, and Cd (45%–60%). This suggests that substantial quantities of contaminated soil might be economically treated in a single, real-scale stage, which is unusual for a soil washing procedure. This initial success makes it feasible to envisage subsequent rewashing cycles aiming for a complete soil treatment.

Finally, we have demonstrated that attributive analysis can provide a quality index to establish an optimal separation voltage. According to this analysis, optimal concentrations for the PTEs tested are obtained at 41.5 kV. We suggest that programmes for soil remediation should make use of this mathematical procedure to improve outcomes. Further quotients could be included in this methodology to take account of not only separation performance but also environmental and economic aspects so incorporating the concept of the circular economy into soil remediation operations.

CRediT authorship contribution statement

X. Corres: Conceptualization and design, Investigation, Data curation, Writing – original draft. **D. Baragaño:** Methodology, Data curation. **J.M. Menéndez-Aguado:** Methodology, Investigation. **J.R. Gallego:** Conceptualization and design, Methodology, Funding acquisition. **C. Sierra:** Conceptualization, Data curation, Formal analysis, Writing - Original Draft, Writing – review & editing.

Declaration of competing interest

The authors declare that they have no known competing financial interests or personal relationships that could have appeared to influence the work reported in this paper.

Data availability

Data will be made available on request.

Funding

Diego Baragaño would like to express his gratitude to the European Union-Next Generation EU, the Spanish Ministry of Universities, and The Recovery, Transformation and Resilience Plan for providing the funding for his postdoctoral grant which was administered by the University of Oviedo (Ref. MU-21-UP2021-03032892642). Carlos Sierra thanks the EURECA-PRO phase I 2020–2023 co-funded by the Erasmus+ Programme of the European Union (Ref.: 101004049).

Appendix A. Supplementary data

Supplementary material related to this article can be found online at https://doi.org/10.1016/j.eti.2023.103237.

References

Adamo, P., Dudka, S., Wilson, M.J., McHardy, W.J., 1996. Chemical and mineralogical forms of cu and Ni in contaminated soils from the sudbury mining and smelting region, Canada. Environ. Pollut. 91 (1), 11–19. http://dx.doi.org/10.1016/0269-7491(95)00035-P.

Aitani, A.M., 2004. Oil refining and products. Encycl. Energy 71, 5–729, https://www.academia.edu/21206560/Oil_Refining_and_Products.

Anderson, R., Rasor, E., van Ryn, F., 1999. Particle size separation via soil washing to obtain volume reduction. J. Hard Mater. 66 (1–2), 89–98. http://dx.doi.org/10.1016/S0304-3894(98)00210-6.

Baragaño, D., Berrezueta, E., Komárek, M., Menéndez-Aguado, J.M., 2023. Magnetic separation for arsenic and metal recovery from polluted sediments within a circular economy. J. Env. Manag. 339, 117884. http://dx.doi.org/10.1016/j.jenvman.2023.117884.

Baragaño, D., Gallego, J.L.R., María Menéndez-Aguado, J., Marina, M.A., Sierra, C., 2021. As sorption onto fe-based nanoparticles and recovery from soils by means of wet high intensity magnetic separation. Chem. Eng. J. 408, 127325. http://dx.doi.org/10.1016/J.CEJ.2020.127325.

Bedeković, G., Trbović, R., 2020. Electrostatic separation of aluminium from residue of electric cables recycling process. Waste Manage. 108, 21–27. http://dx.doi.org/10.1016/j.wasman.2020.04.033.

Beiyuan, J., Tsang, D.C.W., Valix, M., Baek, K., Ok, Y.S., Zhang, W., Bolan, N.S., Rinklebe, J., Li, X.D., 2018. Combined application of EDDS and EDTA for removal of potentially toxic elements under multiple soil washing schemes. Chemosphere 205, 178–187. http://dx.doi.org/10.1016/J.CHEMOSPHERE.2018.04.081.

Buchman, M., Office of Response, N., 2008. SQuiRT cards. (n.d.).

Dermont, G., Bergeron, M., Mercier, G., Richer-Laflèche, M., 2008. Soil washing for metal removal: A review of physical/chemical technologies and field applications. J. Hard Mater. 152 (1), 1–31. http://dx.doi.org/10.1016/J.JHAZMAT.2007.10.043.

EEA, 2009. Overview of Economic Activities Causing Soil Contamination in Some WCE and SEE Countries. European Environment Agency (EEA), https://www.eea.europa.eu/data-and-maps/figures/overview-of-economic-activities-causing-soil-contamination-in-some-wce-and-see-countries-pct-of-investigated-sites.

Feng, W., Zhang, S., Zhong, Q., Wang, G., Pan, X., Xu, X., Zhou, W., Li, T., Luo, L., Zhang, Y., 2020. Soil washing remediation of heavy metal from contaminated soil with EDTMP and PAA: Properties, optimization, and risk assessment. J. Hard Mater. 381, 120997. http://dx.doi.org/10.1016/J.JHAZMAT.2019.120997.

França, F.C.S.S., Albuuerque, A.M.A., Almeida, A.C., Silveira, P.B., Filho, C.A., Hazin, C.A., Honorato, E. v., 2017. Heavy metals deposited in the culture of lettuce (Lactuca sativa L.) by the influence of vehicular traffic in pernambuco, Brazil. Food Chem. 215, 171–176. http://dx.doi.org/10.1016/J.FOODCHEM.2016.07.168.

Gu, Y., Yeung, A.T., Li, H., 2018. Enhanced electrokinetic remediation of cadmium-contaminated natural clay using organophosphonates in comparison with EDTA. Chin. J. Chem. Eng. 26 (5), 1152–1159. http://dx.doi.org/10.1016/J.CJCHE.2017.10.012.

Inculet, I.I., 1984. Electrostatic mineral separation. p. 153, https://books.google.com/books/about/Electrostatic_Mineral_Separation.html?hl=es&id=m_XmAAAAMAAJ.

Kawatra, S.K., Young, C., 2019. SME Mineral Processing & Extractive Metallurgy HandBook. p. 2203.

Kdidi, S., Vaca-Medina, G., Peydecastaing, J., Oukarroum, A., Fayoud, N., Barakat, A., 2019. Electrostatic separation for sustainable production of rapeseed oil cake protein concentrate: Effect of mechanical disruption on protein and lignocellulosic fiber separation. Powder Technol. 344, 10–16. http://dx.doi.org/10.1016/j.powtec.2018.11.107.

Khalid, S., Shahid, M., Niazi, N.K., Murtaza, B., Bibi, I., Dumat, C., 2017. A comparison of technologies for remediation of heavy metal contaminated soils. J. Geochem. Explor. 182, 247–268. http://dx.doi.org/10.1016/J.GEXPLO.2016.11.021.

Li, Q., Guo, L., Cao, H., Li, A., Xu, W., Wang, Z., 2021. Effects of an effective adsorption region on removing catalyst particles from an FCC slurry under a DC electrostatic field. Powder Technol. 377, 676–683. http://dx.doi.org/10.1016/j.powtec.2020.09.038.

Li, Y., Liao, X., Li, W., 2019a. Combined sieving and washing of multi-metal-contaminated soils using remediation equipment: A pilot-scale demonstration. J. Clean. Prod. 212, 81–89. http://dx.doi.org/10.1016/J.JCLEPRO.2018.11.294.
Li, X., Thornton, I., 2001. Chemical partitioning of trace and major elements in soils contaminated by mining and smelting activities. Appl. Geochem. 16 (15), 1693–1706. http://dx.doi.org/10.1016/S0883-2927(01)00065-8.
Li, Q., Zhang, Z., Wu, Z., Wang, Z., Guo, L., 2019b. Effects of electrostatic field and operating parameters on removing catalytic particles from FCCS. Powder Technol. 342, 817–828. http://dx.doi.org/10.1016/j.powtec.2018.10.060.
Lillo Ramos, F.J., 1992. Geology and geochemistry of linares-la carolina pb-ore field (southeastern border of the hesperian massif).
Loredo, J., Ordóñez, A., Gallego, J.R., Baldo, C., García-Iglesias, J., 1999. Geochemical characterisation of mercury mining spoil heaps in the area of mieres (asturias, northern Spain). J. Geochem. Explor. 67 (1–3), 377–390. http://dx.doi.org/10.1016/S0375-6742(99)00066-7.
Lorite, I.J., Castilla, A., Cabezas, J.M., Alza, J., Santos, C., Porras …, R., Sillero, J.C., 2023. Analyzing the impact of extreme heat events and drought on wheat yield and protein concentration, and adaptation strategies using long-term cultivar trials under semi-arid conditions. Agricult. Forest Meteorol. 329, 109279. http://dx.doi.org/10.1016/j.agrformet.2022.109279.
Makino, T., Sugahara, K., Sakurai, Y., Takano, H., Kamiya, T., Sasaki, K., Itou, T., Sekiya, N., 2006. Remediation of cadmium contamination in paddy soils by washing with chemicals: Selection of washing chemicals. Environ. Pollut. 144 (1), 2–10. http://dx.doi.org/10.1016/J.ENVPOL.2006.01.017.
Martínez, J., Llamas, J., de Miguel, E., Rey, J., Hidalgo, M.C., 2007a. Determination of the geochemical background in a metal mining site: example of the mining district of linares (south Spain). J. Geochem. Explor. 94 (1–3), 19–29. http://dx.doi.org/10.1016/j.gexplo.2007.05.001.
Martínez, J., Llamas, J.F., de Miguel, E., Rey, J., Hidalgo, M.C., 2007b. Application of the visman method to the design of a soil sampling campaign in the mining district of linares (Spain). J. Geochem. Explor. 92 (1), 73–82. http://dx.doi.org/10.1016/j.gexplo.2006.07.004.
Martínez, J., Rey, J., Hidalgo, M.C., Benavente, J., 2012. Characterizing abandoned mining dams by geophysical (ERI) and geochemical methods: The linares-la carolina district (southern Spain). Water Air Soil Pollut. 223 (6), 2955–2968. http://dx.doi.org/10.1007/s11270-012-1079-7.
Park, C.H., Subasinghe, N., Jeon, H.S., 2015. Separation of covering plastics from particulate copper in cable wastes by induction electrostatic separation. Mater. Trans. 56 (7), 1140–1143. http://dx.doi.org/10.2320/matertrans.M2015138.
Pfeifroth, Uwe, Kothe, Steffen, Müller, Richard, Trentmann, Jörg, Hollmann, Rainer, Fuchs, Petra, Werscheck, Martin, 2017. Surface Radiation Data Set - Heliosat (SARAH) - Edition 2. Satellite Application Facility on Climate Monitoring, http://dx.doi.org/10.5676/EUM_SAF_CM/SARAH/V002.
Piccolo, A., Spaccini, R., de Martino, A., Scognamiglio, F., di Meo, V., 2019. Soil washing with solutions of humic substances from manure compost removes heavy metal contaminants as a function of humic molecular composition. Chemosphere 225, 150–156. http://dx.doi.org/10.1016/J.CHEMOSPHERE.2019.03.019.
Rui, D., Wu, Z., Ji, M., Liu, J., Wang, S., Ito, Y., 2019. Remediation of Cd- and Pb- contaminated clay soils through combined freeze-thaw and soil washing. J. Hard Mater. 369, 87–95. http://dx.doi.org/10.1016/J.JHAZMAT.2019.02.038.
Sierra, C., Gallego, J.R., Afif, E., Menéndez-Aguado, J.M., González-Coto, F., 2010. Analysis of soil washing effectiveness to remediate a brownfield polluted with pyrite ashes. J. Hard Mater. 180 (1–3), 602–608. http://dx.doi.org/10.1016/j.jhazmat.2010.04.075.
Sierra, C., Martínez, J., Menéndez-Aguado, J.M., Afif, E., Gallego, J.R., 2013. High intensity magnetic separation for the clean-up of a site polluted by lead metallurgy. J. Hazard. Mater. 248–249 (1), 194–201. http://dx.doi.org/10.1016/j.jhazmat.2013.01.011.
Tabtabaei, S., Konakbayeva, D., Rajabzadeh, A.R., Legge, R.L., 2019. Functional properties of navy bean (phaseolus vulgaris) protein concentrates obtained by pneumatic tribo-electrostatic separation. Food Chem. 283, 101–110. http://dx.doi.org/10.1016/j.foodchem.2019.01.031.
Tabtabaei, S., Vitelli, M., Rajabzadeh, A.R., Legge, R.L., 2017. Analysis of protein enrichment during single- and multi-stage tribo-electrostatic bioseparation processes for dry fractionation of legume flour. Sep. Purif. Technol. 176, 48–58. http://dx.doi.org/10.1016/j.seppur.2016.11.050.
Uchimiya, M., Wartelle, L.H., Klasson, K.T., Fortier, C.A., Lima, I.M., 2011. Influence of pyrolysis temperature on biochar property and function as a heavy metal sorbent in soil. J. Agricult. Food Chem. 59 (6), 2501–2510. http://dx.doi.org/10.1021/JF104206C/SUPPL_FILE/JF104206C_SI_001.PDF.
Villot, A., Gonthier, Y., Gonze, E., Bernis, A., Ravel, S., Grateau, M., Guillaudeau, J., 2012. Separation of particles from syngas at high-temperatures with an electrostatic precipitator. Sep. Purif. Technol. 92, 181–190. http://dx.doi.org/10.1016/j.seppur.2011.04.028.
Wang, G., Zhang, S., Zhong, Q., Xu, X., Li, T., Jia, Y., Zhang, Y., Peijnenburg, W.J.G.M., Vijver, M.G., 2018. Effect of soil washing with biodegradable chelators on the toxicity of residual metals and soil biological properties. Sci. Total Environ. 625, 1021–1029. http://dx.doi.org/10.1016/J.SCITOTENV.2018.01.019.
Wills, B.A., Napier-Munn, T.J., 2006. Mineral processing technology: An introduction to the practical aspects of ore treatment and mineral recovery. In: Butterworth-Heinemann (Ed.), Wills' Mineral Processing Technology, seventh ed. Butterworth-Heinemann, http://dx.doi.org/10.1016/C2010-0-65478-2.
Wu, Q., Leung, J.Y.S., Geng, X., Chen, S., Huang, X., Li, H., Huang, Z., Zhu, L., Chen, J., Lu, Y., 2015. Heavy metal contamination of soil and water in the vicinity of an abandoned e-waste recycling site: Implications for dissemination of heavy metals. Sci. Total Environ. 506–507, 217–225. http://dx.doi.org/10.1016/J.SCITOTENV.2014.10.121.
Xu, J., Kleja, D.B., Biester, H., Lagerkvist, A., Kumpiene, J., 2014. Influence of particle size distribution, organic carbon, pH and chlorides on washing of mercury contaminated soil. Chemosphere 109, 99–105. http://dx.doi.org/10.1016/J.CHEMOSPHERE.2014.02.058.
Yang, X., Wang, H., Peng, Z., Hao, J., Zhang, G., Xie, W., He, Y., 2018. Triboelectric properties of ilmenite and quartz minerals and investigation of triboelectric separation of ilmenite ore. Int. J. Mining Sci. Technol. 28 (2), 223–230. http://dx.doi.org/10.1016/j.ijmst.2018.01.003.
Zhao, L., Ding, Z., Sima, J., Xu, X., Cao, X., 2017. Development of phosphate rock integrated with iron amendment for simultaneous immobilization of Zn and Cr (VI) in an electroplating contaminated soil. Chemosphere 182, 15–21. http://dx.doi.org/10.1016/J.CHEMOSPHERE.2017.05.004.